



Fos expression in neurons of the rat vestibulo-autonomic pathway activated by sinusoidal galvanic vestibular stimulation

Gay R. Holstein^{1,2,3*}, Victor L. Friedrich Jr.², Giorgio P. Martinelli¹, Dmitri Ogorodnikov¹, Sergei B. Yakushin¹ and Bernard Cohen¹

¹ Department of Neurology, Mount Sinai School of Medicine, New York, NY, USA

² Department of Neuroscience, Mount Sinai School of Medicine, New York, NY, USA

³ Department of Anatomy/Functional Morphology, Mount Sinai School of Medicine, New York, NY, USA

Edited by:

Kenna Peusner, George Washington University, USA

Reviewed by:

Kenna Peusner, George Washington University, USA

Hans Straka, LMU Munich, Germany

*Correspondence:

Gay R. Holstein, Department of Neurology, Mount Sinai School of Medicine, One Gustave Levy Place, Box 1140, New York, NY 10029, USA.
e-mail: gay.holstein@mssm.edu

The vestibular system sends projections to brainstem autonomic nuclei that modulate heart rate and blood pressure in response to changes in head and body position with regard to gravity. Consistent with this, binaural sinusoidally modulated galvanic vestibular stimulation (sGVS) in humans causes vasoconstriction in the legs, while low frequency (0.02–0.04 Hz) sGVS causes a rapid drop in heart rate and blood pressure in anesthetized rats. We have hypothesized that these responses occur through activation of vestibulo-sympathetic pathways. In the present study, c-Fos protein expression was examined in neurons of the vestibular nuclei and rostral ventrolateral medullary region (RVLM) that were activated by low frequency sGVS. We found c-Fos-labeled neurons in the spinal, medial, and superior vestibular nuclei (SpVN, MVN, and SVN, respectively) and the parasolitary nucleus. The highest density of c-Fos-positive vestibular nuclear neurons was observed in MVN, where immunolabeled cells were present throughout the rostro-caudal extent of the nucleus. c-Fos expression was concentrated in the parvocellular region and largely absent from magnocellular MVN. c-Fos-labeled cells were scattered throughout caudal SpVN, and the immunostained neurons in SVN were restricted to a discrete wedge-shaped area immediately lateral to the IVth ventricle. Immunofluorescence localization of c-Fos and glutamate revealed that approximately one third of the c-Fos-labeled vestibular neurons showed intense glutamate-like immunofluorescence, far in excess of the stain reflecting the metabolic pool of cytoplasmic glutamate. In the RVLM, which receives a direct projection from the vestibular nuclei and sends efferents to preganglionic sympathetic neurons in the spinal cord, we observed an approximately threefold increase in c-Fos labeling in the sGVS-activated rats. We conclude that localization of c-Fos protein following sGVS is a reliable marker for sGVS-activated neurons of the vestibulo-sympathetic pathway.

Keywords: otolith organs, blood pressure, heart rate, orthostatic hypotension, vasovagal syncope, sympathetic nervous system, vestibular nuclei, rostral ventrolateral medulla

INTRODUCTION

The family of immediate early genes has over 40 members, including *c-fos*, *c-jun*, and *c-myc*. Many of the genes in this family, including *c-fos*, are DNA-binding transcription factors with a zinc finger motif (Curran and Morgan, 1995). The protein product of *c-fos* activation, c-Fos, is transported to the cell nucleus, where it dimerizes with members of the Jun protein family to form activator protein (AP)-1 transcriptional complexes. Such complexes, in turn, participate in the subsequent regulation of target (late) gene expression (for reviews, see Morgan and Curran, 1991; Hughes and Dragunow, 1995; Durchdewald et al., 2009).

Immediate early genes have minimal expression in quiescent neurons, but are transiently activated in response to a broad spectrum of excitatory extracellular stimuli. Of note, the intracellular signaling cascades triggered by such stimuli occur over a more protracted period (minutes–hours) than the millisecond timeframe of

synaptically mediated changes in neuronal excitability (Illing et al., 2002). In fact, peak *c-fos* mRNA and c-Fos protein accumulation occur approximately 30 min and 1.5–4 h following stimulation, respectively, and protein levels usually return to baseline within 6–8 h (Morgan and Curran, 1989; Herdegen and Leah, 1998). Since *c-fos* transcription is relatively rapid, does not require new protein synthesis, and has a very short half-life, and since the protein product has a high turnover rate, gene expression and c-Fos protein accumulation can be used as indicators of neuronal activity (Morgan and Curran, 1991). Moreover, since induction of *c-fos* mRNA and accumulation of c-Fos protein can occur trans-synaptically, it is possible to identify functionally related neurons at multiple stages along neural pathways of interest (Dragunow and Faull, 1989). While the extended period of c-Fos protein accumulation precludes the possibility of identifying sequential synaptic connections based on temporal dissection, as is done with viral vector

tracing techniques, the advantage of *c-Fos* localization is the ability to visualize neurons that are specifically activated by a particular stimulus.

The utility of *c-Fos* as a marker for neuronal activation has been demonstrated in a wide range of studies using behavioral paradigms, systemic drug infusions, neuroreceptor ligand binding, and electrical and chemical stimulation (Herdegen and Leah, 1998). Fos expression has typically been associated with excitatory activation of sensory systems, and *c-Fos* is not manifest in neurons that are tonically inhibited (Chan and Sawchenko, 1994). Cells that receive predominantly excitatory input and some cells under conditions of release from tonic inhibition show *c-Fos* expression in response to stimulation, although other disinhibited neurons do not (for review, see Kovács, 2008). Moreover, *c-Fos* is rarely observed in large motor neurons of the brainstem (Chan and Sawchenko, 1994). Thus, *c-Fos* expression occurs only in a subset of the cells that are activated by a particular stimulus.

In the vestibular system, *c-fos* expression and *c-Fos* protein localization have been used to visualize neurons that participate in several functional pathways and systems-level mechanisms. These studies have sought to identify the locations and distributions of neurons activated by semicircular canal, otolith organ, or combined canal/otolith-related stimulation achieved through a variety of experimental paradigms including horizontal and vertical linear acceleration, Ferris wheel rotation, off-vertical-axis rotation (OVAR), centrifugation, spaceflight, and steps of galvanic vestibular stimulation (GVS; Kaufman et al., 1992b, 1993; Kaufman and Perachio, 1994; Marshburn et al., 1997; Gustave Dit Duflo et al., 2000; Saxon et al., 2001; Pompeiano et al., 2002; Chen et al., 2003; Fuller et al., 2004; Lai et al., 2004, 2006, 2008; Kaufman, 2005; Zhang et al., 2005; Cai et al., 2007, 2010; Tse et al., 2008; Abe et al., 2009; Baizer et al., 2010). In addition, a number of studies have used *c-Fos* to identify central vestibular neurons that are activated in response to unilateral or bilateral destruction or inactivation of receptor hair cells, individual end organs, the entire labyrinth or the vestibular nerves (Kaufman et al., 1992a, 1993, 1999; Kitahara et al., 1995, 1997; Cirelli et al., 1996; Darlington et al., 1996; Kim et al., 1997, 2002; Gustave Dit Duflo et al., 1999; Shinder et al., 2005a,b, 2006), since these cells and tissues may play key roles in the process of vestibular compensation.

It is well documented in experimental animals that the vestibular system sends projections to autonomic centers that modulate heart rate and blood pressure in response to changes in head and body position, particularly with regard to gravity (for review, see Holstein et al., 2011b). Primary afferents of this pathway are derived mostly (but not exclusively) from the otolith organs, and are thought to terminate on cells in the caudal vestibular nuclear complex (VNC). Second order vestibular neurons project directly as well as indirectly to brainstem sites involved in the regulation of cardiovascular activity such as nucleus tractus solitarius (NTS) and the rostral ventrolateral medullary region (RVLM; Balaban and Beryozkin, 1994; Yates and Miller, 1994; Yates et al., 1994; Porter and Balaban, 1997; Holstein et al., 2011a). However, despite the nearly century-old appreciation that the vestibular system participates in the control of blood pressure (Bradbury and Eggleston, 1925), and a wealth of information concerning the baroreflex

pathways, the descending vestibulo-sympathetic pathways remain largely uncharacterized.

Steps of GVS have been used in experimental animals to activate vestibular nerve fibers and cause changes in blood pressure and heart rate (Courjon et al., 1987; Abe et al., 2008, 2009). In addition, GVS has been used extensively in humans, in whom brief trains of sinusoidally modulated GVS (sGVS) have repeatedly been demonstrated to increase muscle sympathetic nerve activity (SNA; Bent et al., 2006; Voustianouk et al., 2006; Grewal et al., 2009; James and Macefield, 2010; James et al., 2010). This current activates the entire vestibular nerve (Peterson et al., 1980; Goldberg et al., 1984), but does not appear to stimulate non-vestibular “graviceptors” (for review, see Curthoys, 2010). Although sGVS initiates activity throughout the VNC, the responses of many activated vestibular neurons habituate rapidly (Courjon et al., 1987). For a more detailed discussion of the impact of sGVS stimulation, please see the accompanying Opinion Article by Cohen and colleagues. In brief, the low frequency of the sinusoidal stimulus, the frequency-dependent postural sway evoked by sGVS in standing human subjects (Lau et al., 2003), and the ocular roll but not nystagmus that is elicited by sGVS (Watson et al., 1998; MacDougall et al., 2005) all suggest the central pathways that remain activated as a result of this stimulus are primarily related to the otolith system. Our recent report of sGVS effects on heart rate and blood pressure in rodents further supports this conclusion (Cohen et al., 2011). The present study tested the hypotheses that the immediate early gene *c-fos* is activated in response to sGVS, and that *c-Fos* protein accumulates in the nuclei of vestibular neurons located in regions that are associated with vestibulo-autonomic pathways in sGVS-stimulated animals, but not in non-stimulated controls.

MATERIALS AND METHODS

All experiments were approved by the Institutional Care and Use Committee of the Mount Sinai School of Medicine and were carried out in accordance with the National Institutes of Health Guide for the Care and Use of Laboratory Animals (NIH Publications No. 80-23, revised 1996). Data from 20 adult, male Long-Evan rats (Harlan Laboratories, MA, USA) weighing 300–400 g were used for these studies. Five rats received head fixation mounts and implanted telemetric transmitters to measure blood pressure. Three rats were used in terminal experiments in which blood pressure was measured via a transducer catheter inserted into the external carotid or femoral artery. These rats were not used for anatomical experiments. In the remaining 12 animals, peripheral blood pressure was measured by photoplethysmography (PPG) and no head mounts were used. PPG is a non-invasive optical technique used to detect blood volume changes at the surface of the skin.

SURGICAL PROCEDURES

All surgical procedures were conducted aseptically in rats anesthetized with isoflurane (4% induction; 2–2.5% maintenance in 95% O₂/5% CO₂), and kept on an Isotherm heating pad regulated by feedback from a rectal thermometer. Post-surgical pain was managed with buprenorphine (0.05 mg/kg BID, SQ) for 3 days. Rats were allowed to recover for a minimum of 7 days before they were used in experiments. Implantation of telemetric blood

pressure measurement devices and placement of head fixation mounts (described below) were accomplished during the same aseptic surgical session.

IMPLANTATION OF HEAD MOUNTS FOR PAINLESS IMMOBILIZATION OF THE HEAD

Rats were anesthetized with isoflurane (as above) and placed in a stereotaxic frame. After removing a round patch of skin and the periosteum from the calvarium, sterile stainless-steel screws were secured into four burr holes drilled around the perimeter of the skull. Dental acrylic cement was poured over the calvarium to cover the screws. Two steel nuts were also encased in the hardening acrylic to receive the bolts used to immobilize the subject's head during some vestibular testing.

IMPLANTATION OF TELEMETRIC BLOOD PRESSURE SENSORS IN THE AORTA

Five rats were implanted with telemetric blood pressure sensors (DSI, St Paul, MN, USA). After placing an approximately 2 cm incision in the groin, the femoral artery was isolated and occluded with two mini-clamps. The sensor catheter was inserted into the vessel via a small arteriotomy and, after removing the cranial clamp, was advanced into the abdominal aorta. The catheter was secured with two ties around the artery and the body of the sensor was placed into a subcutaneous pocket in the animal's flank. The pocket was closed with a purse-string suture and the skin incision was closed with surgical staples. Of the five rats, three received sGVS (see below) and two were used as mock stimulation controls.

CANNULATION OF CAROTID AND FEMORAL ARTERIES

Three rats were used in terminal experiments in which blood pressure was recorded with an external pressure transducer connected to a Grass amplifier. Rats were anesthetized with isoflurane (as above) and placed in a supine position in a stereotaxic frame. In one rat, a transducer catheter was introduced into the femoral artery and advanced into the abdominal aorta. In two other rats, the catheter was placed into the external carotid artery. Blood pressure was measured via Grass amplifier. No anatomical studies were conducted on tissue from these animals.

SINUSOIDAL GALVANIC VESTIBULAR STIMULATION (sGVS)

sGVS was given binaurally in 16 animals (the 6 rats with intra-aortic sensors and 10 rats with no implanted devices) at 2 mA and a frequency of 0.025 Hz. The stimulus was applied for five cycles and repeated five times with 3 min rest between repetitions. Sinusoidal currents generated by a computer-controlled stimulator (Voustianiouk et al., 2004) were delivered via Ag/AgCl needle electrodes (BAK) inserted into the skin over the mastoids, behind the external auditory meati (Cohen et al., 2011).

MOCK STIMULATION CONTROLS

Four rats were used as controls for the sGVS stimulation. Two of these rats had head mounts and implanted telemetric blood pressure sensors, and the other two were tested using PPG. The control rats were placed in the cylindrical holder for sGVS testing. Ag/AgCl needle electrodes were inserted into the skin over the mastoids, behind the external auditory meati, and connected to the current stimulator. The rats were maintained as such for 90–120 min,

but no current was applied. All subsequent animal and tissue treatments were identical for the mock- and sGVS-stimulated subjects.

BLOOD PRESSURE AND HEART RATE MEASUREMENTS

Blood pressure data from the telemetric sensors were collected via a wand receiver (DSI, St Paul, MN, USA). Blood pressure in response to sGVS or mock stimulation was recorded continuously using customized A/D conversion hardware and stored at a rate of 1 KHz with 12-bit resolution (Data Translation, Inc.; Marlboro, MA, USA). The data were converted for analysis using VMF data analysis software.

PHOTOPLETHYSMOGRAPHY

We modified the standard clinical PPG method (Imholtz et al., 1991) in order to assess the heart rate and blood pressure changes induced by sGVS non-invasively. PPG monitors peripheral blood circulation, and the signal is composed of two major factors: peripheral blood pressure and vasoconstriction (Imholtz et al., 1991). The PPG signal was initially processed by a band pass filter in the hardware in order to increase the heart beat component. High frequency noise was removed off-line in the analysis software. PPG was recorded in 12 rats from a small clamp placed on a paw.

TISSUE HARVESTING AND PROCESSING

Perfusion, fixation, and tissue sectioning

While peak c-Fos protein accumulation has been demonstrated 90–240 min after stimulation, most studies report maximal expression at 90–120 min and decreased expression at shorter and longer times (for recent reviews, see Kovács, 2008 #2526; Durchdewald et al., 2009 #2527). On this basis, animals for the present study were deeply anesthetized with isoflurane and perfused transcardially with 100 ml of (37°C) 10 mM phosphate buffered saline (PBS) followed by 500 ml of 4% paraformaldehyde/0.2% glutaraldehyde fixative in 0.1 M PB (pH 7.4) at room temperature (RT) 90 min after the completion of the sGVS stimulation. Brains were harvested immediately after perfusion, blocked using an adult rat brain coronal matrix (Ted Pella, Inc.; Redding, CA, USA), and stored at 4°C in PBS with 0.02% NaN₃. Tissue blocks were subsequently cut by vibrating microtome into 50 μm thick serial sections that extended through the entire VNC and ventrolateral medullary region. All the medullary sections (usually about 120 per animal) were stored in PBS with 0.02% NaN₃ (as a preservative) at 4°C.

Anatomical boundaries

The presence and location of the four main vestibular nuclei (spinal, medial, lateral, and superior) were determined for each tissue section by comparison of the anatomical structures present in the dorsal aspect of the section with the most commonly used stereotaxic atlases of the region (Paxinos and Watson, 1998; Paxinos et al., 1999). The boundaries for the RVLM were determined in each tissue section by comparison of the structures present in the ventral aspect of the section with published maps and atlases of that region (Paxinos et al., 1999; Card et al., 2006; Bourassa et al., 2009; Goodchild and Moon, 2009). Utilizing the most conservative

estimates based on these published maps, we identified the RVLM as the 1-mm rostro-caudal region extending from approximately 11.8 to 12.8 mm caudal to Bregma. The other dimensions of the region were defined by a triangle with pars compacta of nucleus ambiguus at the apex, and the ventral surface of the medulla 1.4 and 2.2 mm lateral to the midline as the two other geometric points. As recently noted (Goodchild and Moon, 2009), this region corresponds well with previously published functional and physiological maps of RVLM. Related nuclear groups such the caudal ventrolateral medulla and the intermediolateral cell column were not analyzed in this study.

Primary antibodies

The monoclonal mouse anti-glutamate (MAb 215B2, IgG1) antibody used in this study was produced in our laboratory. A full description of the antibody production, characterization, and specificity was published previously (Holstein et al., 2004). Antibodies produced by this clone were screened exhaustively by ELISA for cross-reactivity with other amino acids and neurotransmitters conjugated to bovine serum albumin (BSA) by glutaraldehyde. In addition, pre-incubation of MAb 215B2 with glutamate bound to BSA completely blocked ELISA reactivity and tissue section staining. ELISA assays also demonstrated that free glutamate could be fixed to rat brain homogenate protein by the paraformaldehyde/glutaraldehyde mixture (but not by paraformaldehyde alone), and that fixed glutamate was specifically recognized by our anti-glutamate monoclonal antibody (Holstein et al., 2011a).

Four commercial antibodies against c-Fos were utilized in this study: two rabbit polyclonal antisera (Santa Cruz Biotechnology, Cat. #253; Calbiochem, Cat. # PC38), one rabbit polyclonal antiserum directly conjugated with Alexa Fluor 488 (Santa Cruz Biotechnology, Cat. #253 AF488), and one mouse monoclonal IgM antibody (United States Biologicals; Cat. #C-0030-02). In addition, some tissue sections were exposed to a mixture of rabbit polyclonal antibody (Santa Cruz Biotechnology, Cat. #253) preabsorbed with blocking peptide as a control for non-specific staining. With our tissue fixation and processing conditions, the unlabeled polyclonal sera provided more robust labeling than the monoclonal antibody and the Alexa Fluor 488-tagged polyclonal antiserum. Results using the two unlabeled polyclonal sera were indistinguishable.

A commercial mouse monoclonal antibody against tyrosine hydroxylase (TH; Millipore, Billerica, MA, USA) was also utilized in the research. This antibody was used to identify catecholaminergic neurons in the RVLM, and stained the same catecholaminergic cell groups, including the C1 group, demonstrated by other investigators (Armstrong et al., 1982).

Reagents

Primary and secondary antibodies were diluted in blocking buffer (ADB: PBS containing 10% normal goat serum, 0.1% Triton X-100, and 0.02% NaN_3). Streptavidins were diluted in PBS containing 0.5% BSA (Sigma, Cat. #A7530, St. Louis, MO, USA) and 0.1% gelatin (PBG; Type A from porcine skin; Sigma). NaN_3 was omitted from buffers used to dilute peroxidase-labeled secondary reagents.

Immunofluorescence

Tissue sections were processed for multiple-label immunofluorescence detection of c-Fos, glutamate, and TH, as well as DAPI staining to visualize the location and size of neuronal nuclei. All steps were performed at RT with agitation on an orbital shaker. Free-floating sections were pre-incubated for 3–6 h in ADB; incubated for 12–18 h in ADB containing primary antibodies; washed for 4–8 h in multiple changes of PBS; incubated for 12–18 h in ADB containing mixed species- or IgG subclass-specific biotin- or Alexa Fluor-conjugated secondary antibodies; washed for 4–8 h in multiple changes of PBS, and immersed in DAPI solution (300 nM in PBS) for 30 min. After the final washes, all sections were mounted on glass slides and coverslipped using Prolong (Invitrogen) as a mounting medium.

The multiple-label immunofluorescence experiments utilized combinations of primary antibodies distinguished by their host species (mouse anti-glutamate, rabbit or mouse anti-c-Fos, rabbit anti-TH), immunoglobulin class and subclass. Secondary antibodies were applied as mixtures of species- and isotype-specific reagents selected such that each secondary recognized only one component of the primary antibody mixture. Primary reagents were always pre-mixed and added concurrently and, after thorough washing, all secondary antibodies were also pre-mixed and applied simultaneously.

Crosstalk among the secondary antibodies was assessed by applying each secondary to sections labeled with the inappropriate primary reagent (e.g., goat anti-mouse secondary following a rabbit anti-c-Fos primary antiserum). Each secondary antibody bound only to its appropriate primary antibody, with negligible binding to inappropriate primaries. In addition, most of the cellular elements that were present in the immunofluorescence-stained sections were stained by only one of the colors in the specimen's secondary mixture. This provides an indication within single sections that only one secondary antibody bound to each primary antibody, and therefore that secondary antibody cross-reactivity was insignificant.

Since we have experienced varying degrees of sensitivity among secondary antibodies, we used several alternative secondary antibodies and several alternative fluorochromes to detect each primary antibody. Consequently, our staining protocols include the same combination of primary antibodies visualized using several different combinations of secondaries, including Alexa Fluors 350, 488, 532, 568, and 647 (Invitrogen).

Immunoperoxidase/diaminobenzidine staining

Vibratome sections were blocked with ADB (4–6 h) and treated with anti-c-Fos antibody (12–18 h) followed by PBS rinses (six changes over 4–6 h) and either biotinylated secondary antibody (12–18 h), PBS rinses (six changes over 4–6 h), and streptavidin–HRP, or by direct HRP-conjugated secondary antibody. Sections were then rinsed in PBS (six changes over 2 h), and incubated in Tris buffer (pH 7.6) containing 0.5 mg/ml diaminobenzidine (DAB; Sigma D-5905; St. Louis, MO, USA) with 0.01% H_2O_2 .

Microscopy, stain analysis, and image preparation

Sections were examined and images were acquired with a Zeiss Axioplan2 microscope equipped for structured illumination

(ApoTome). The intensity of *c-Fos* staining in different subsets of labeled neurons was not compared or quantified in the sGVs-stimulated animals because stain intensities levels were not calibrated in this study. Quantitative estimates were based on counts of all labeled neuronal nuclei in peroxidase DAB-stained sections. Immunofluorescence labeled tissue was not used for these estimates because peroxidase–DAB is, in general, a more highly sensitive approach.

Publication images were prepared using Adobe Photoshop and Illustrator CS4. Adjustments of brightness and contrast were accomplished with the Photoshop Levels and Curves tools, applied equally to all parts of each image. For these latter adjustments, the levels intensity check function was used to optimize the image data range by clipping the background field to full intensity and the darkest values just above zero. The curves tool was then used to optimize contrast and tonal mapping. The levels tool was then used again, solely as a diagnostic, to double check for clipping regions. Note that we do not use the Photoshop Autolevels function since this imprecisely uses percentages to judge clipping levels.

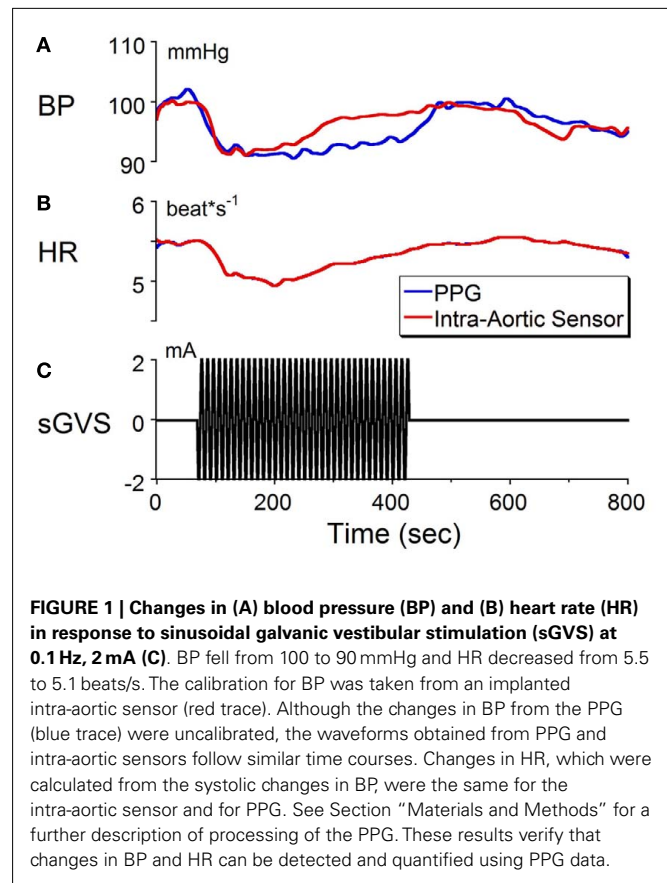
Atlas data

Labeling patterns were plotted using a standard rat brain atlas for reference (Paxinos et al., 1999). Sections stained by immunoperoxidase or immunofluorescence for visualization of *c-Fos* were either examined directly with the microscope or through digital photomicrographs and the locations of labeled cell bodies and axonal arbors were plotted manually on brainstem drawings made from the atlas. The resulting data were then rendered using Adobe Illustrator to produce **Figure 4**.

RESULTS

SINUSOIDAL GVS

We recently reported that binaural sGVs can cause a sudden reduction in blood pressure and heart rate in anesthetized rats (Cohen et al., 2011). These induced vasovagal-like responses have two components, a transient drop in blood pressure that spontaneously recovers over several minutes and oscillations in blood pressure and heart rate that occur at twice the frequency of stimulation. The oscillations persist for the duration of stimulation, and are best induced at frequencies between 0.02 and 0.04 Hz although typical vasovagal responses can be induced at higher frequencies as well. The transient components in blood pressure and heart rate are shown in **Figure 1** in response to stimulation at 0.1 Hz, 2 mA of binaural sGVs in a susceptible rat. Although the gain of the normalized baseline blood pressure derived from the PPG was not of the same magnitude as that derived from the intra-aortic sensor, both signals behaved similarly (**Figures 1A,C**). That is, the averaged blood pressure waveform from the PPG followed the changes in the blood pressure waveform from the intra-aortic sensor. The calibrations for heart rate (**Figures 1B,C**) apply to both the data obtained from the intra-aortic sensor and PPG. Because both signals were derived from the systolic changes in blood pressure, the heart rate from both sensors was identical. Thus, the PPG provided an accurate measure of blood pressure and an accurate reflection of heart rate. These results provide verification that changes in blood pressure and heart rate can be detected and quantified using PPG data. Based on these findings, we utilized PPG to assess heart rate



and blood pressure in animals used for the anatomical studies in order to verify that the sGVs stimulus was effective in causing an autonomic effect prior to tissue harvesting.

c-FOS ACTIVATION

Brainstem sections through the VNC were immunolabeled for detection of *c-Fos* protein in order to visualize neurons of the vestibulo-autonomic pathway that are activated by sGVs. Our initial studies addressed the specificity of *c-Fos* protein accumulation in the tissue. Sets of representative vibratome sections from stimulated (**Figures 2A,B**) and mock (non)stimulated (**Figures 2C,D**) rats were selected as anatomically matched pairs. Each full skip-serial set spanned the entire rostro-caudal extent of the VNC, with 250 μm between sequential sections. The sections from the two groups of rats were processed through the peroxidase–DAB immunolabeling protocol contemporaneously, using the same reagents and incubation periods. The glass slide-mounted tissue sections were imaged using identical photomicroscopic conditions, and the image files were processed using the same decision rules for adjustment of image brightness and contrast. In the mock sGVs-stimulated rats, *c-Fos* protein immunolabel was apparent in the nuclei of some neurons in NTS, the gigantocellular reticular nucleus, nucleus ambiguus, and the RVLM. The few nuclei that were immunolabeled in the vestibular nuclei of the non-stimulated rats (**Figures 2C,D**) were scattered throughout the VNC region, showed no preferential localization within the VNC,

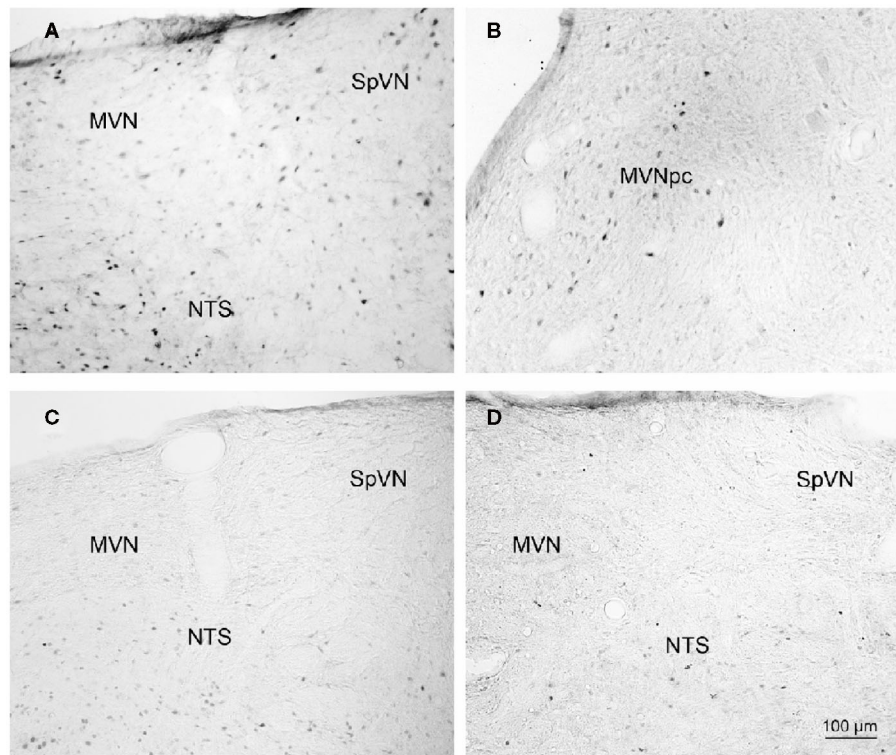


FIGURE 2 | Representative vibratome sections through the vestibular nuclei from two sGVS-stimulated (A,B) and two mock (non)stimulated (C,D) rats processed for immunoperoxidase/diaminobenzidine staining of c-Fos protein. c-Fos-immunoreactive neuronal nuclei are apparent in the

spinal and medial vestibular nuclei (SpVN, MVN), as well as nucleus tractus solitarius (NTS), of the stimulated animals. Sections from the mock-stimulated animals contained c-Fos-labeled cells in NTS, but rarely in the vestibular nuclei. Scale bar in (D) is for all panels.

and comprised fewer than three cells/region/DAB-stained section. Additional tissue sections processed as controls for non-specific staining of the primary and secondary reagents showed no specific labeling (Figure 3). In all sections, staining was restricted to the nuclei of neurons and was not present in the cytoplasm.

DISTRIBUTION OF sGVS-ACTIVATED NEURONS IN THE VESTIBULAR NUCLEI

Series' of vibratome sections from sGVS-stimulated rats were processed for peroxidase–DAB immunocytochemistry to map the distributions of activated, c-Fos-positive neurons throughout the VNC. Since the sequential sections in each series were separated by 250 µm, there was no possibility that the same neuron was present in more than one tissue section of a given series. Stained neuronal nuclei in the VNC of each animal were plotted on standardized stereotaxic atlas templates, based on analysis of brightfield images of each tissue section. These distribution maps demonstrated that sGVS-activated neurons were present in the spinal, medial, and superior vestibular nuclei (SpVN, MVN, and SVN, respectively), as well as the parasolitary nucleus, but not in the lateral vestibular nucleus (LVN). Although there was some variability in the extent of the staining across animals, the localization of activated neurons within the VNC was consistent across all sGVS-stimulated rats ($n = 13$). An example of the distribution of c-Fos immunolabel in the VNC of an sGVS-stimulated rat is shown in Figure 4.

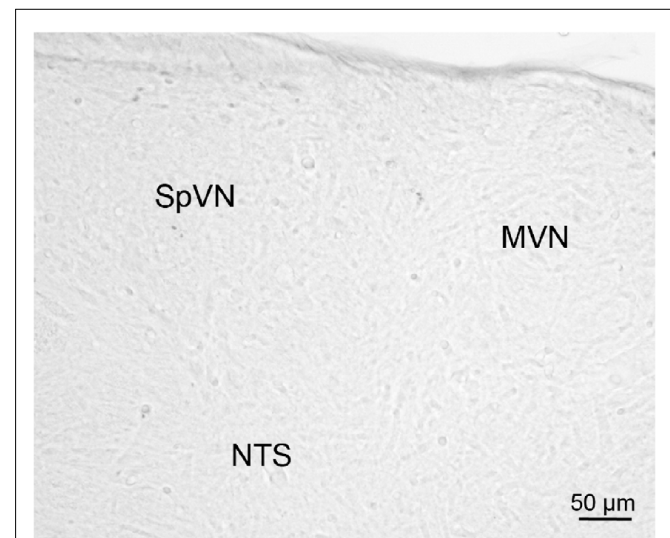


FIGURE 3 | A vibratome section through the caudal vestibular nuclei from an sGVS-stimulated rat, stained with anti-c-Fos antibody pre-incubated with a peptide blocker and then further processed for immunoperoxidase/diaminobenzidine staining. Signal was negligible in such control sections, and in those in which primary and/or secondary reagents were omitted from the processing protocol.

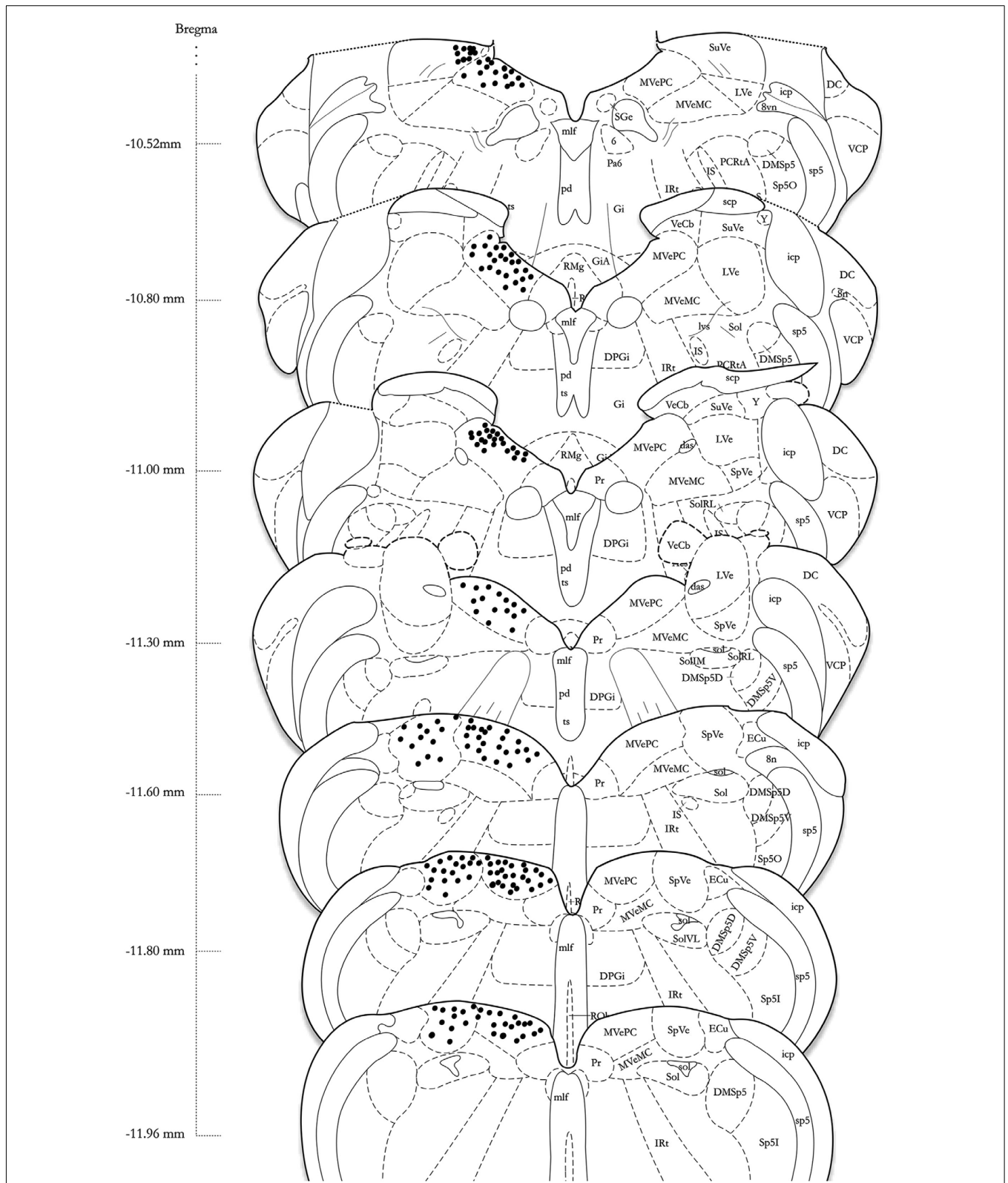


FIGURE 4 | A schematic representation of the distribution of c-Fos-positive cells in the vestibular nuclear complex of one rat following sGVs (see Materials and Methods for details) is shown on the left side of the atlas sections (modified from Paxinos and Watson, 1998). The highest

overall density of immunostained neurons was present in the medial vestibular nucleus (MVN). These cells were localized almost exclusively in the parvocellular region (MVNpc) and caudal MVN. Immunopositive neurons were (Continued)

FIGURE 4 | Continued

present throughout the caudal half of the spinal vestibular nucleus (SpVN), and there was a small dense cluster of immunopositive neurons in the superior vestibular nucleus (SVN). Only labeling in the vestibular nuclei is plotted on this schematic. Approximate Bregma coordinates from the published atlas are indicated to the left. Abbreviations: 6, abducens nucleus; 8vn, vestibular nerve; 8n, vestibulo-cochlear nerve; das, dorsal acoustic stria; DC, dorsal cochlear nucleus; DMSp5, dorsomedial spinal trigeminal nucleus (dorsal D and ventral V subdivisions); DPGi, dorsal paragigantocellular nucleus; ECu, external cuneate nucleus; Gi, nucleus reticularis gigantocellularis; GiA, n. reticularis gigantocellularis, alpha nucleus; icp, inferior cerebellar peduncle; IRt, intermediate reticular nucleus; IS, inferior salivatory nucleus; LVe, lateral

vestibular nucleus; lvs, lateral vestibulo-spinal tract; mlf, medial longitudinal fasciculus; MVeMC, medial vestibular nucleus, magno-cellular division; MVePC, medial vestibular nucleus, parvocellular division; Pa6, paraabducens nucleus; PCrTA, parvicellular reticular nucleus; pd, predorsal bundle; Pr, prepositus nucleus; py, pyramids; RMg, raphé magnus; RVL, rostral ventrolateral medulla; scp, superior cerebellar peduncle; SGe, supragenual nucleus; sol, solitary tract; Sol, solitary nucleus (ventrolateral VL, rostralateral RL, and medial M subdivisions); sp5, spinal trigeminal tract (oral O and interstitial I subdivisions); Sp5l, spinal trigeminal nucleus, pars interpolaris; SpVe, spinal (inferior) vestibular nucleus; SuVe, superior vestibular nucleus; ts, tectospinal tract; VCP, ventral cochlear nucleus, posterior division; VeCb, vestibulocerebellar nucleus; Y, Y-group.

The highest density of *c-Fos*-positive VNC neurons was observed in the MVN, where immunopositive cells were distributed throughout the entire rostro-caudal extent of the nucleus (**Figures 5A–F**). Labeled cells were concentrated in the parvocellular and caudal regions of MVN, but were not preferentially localized in the periventricular zone and were rare in magno-cellular MVN (**Figures 5A,B,D**). *c-Fos*-labeled cells were scattered throughout the caudal half of SpVN (**Figures 5D–F**), whereas the stained neurons in SVN were only present in a discrete wedge-shaped area of the shell (parvocellular) area of the nucleus, immediately lateral to the lateral wings of the IVth ventricle at approximately Bregma -10.52 (**Figure 4**).

MORPHOLOGIC FEATURES OF sGVS-ACTIVATED NEURONS IN THE VESTIBULAR NUCLEI

In order to better visualize the sGVS-activated neurons within the context of VNC chemoanatomy, series' of vibratome sections from the same animals utilized for peroxidase–DAB immunocytochemistry were processed for multiple-label immunofluorescence detection of *c-Fos* with glutamate and the nuclear stain DAPI. There were no differences between the regional localization and distribution of neurons stained by immunofluorescence and by immunoperoxidase–DAB. The immunofluorescence sections verified that the sGVS-activated neurons were located predominantly in caudal and parvocellular MVN (**Figures 6A–C**) and the parasolitary nucleus (**Figure 6C**). Such cells frequently clustered in small groups of 8–12 neurons, which often formed dorsoventrally oriented columns (**Figures 6A,C**). Approximately one third of the *c-Fos*-labeled cells throughout the VNC showed intense glutamate immunostain; the remaining activated neurons showed only trace levels of immunofluorescence that presumably reflect the metabolic pool of cytoplasmic glutamate (**Figure 7A**). Three morphological types of activated neurons were observed: globular (**Figure 7B**), multipolar (**Figure 7C**), and fusiform (**Figure 7D**). The same three morphological cell types send direct projections from the vestibular nuclei to the RVLM (Holstein et al., 2011a). Of these, small diameter globular cells were the predominant *c-Fos*-labeled cytology.

sGVS-ACTIVATED NEURONS IN THE RVLM

One major target of vestibular efferents to autonomic nuclei is a direct projection to the RVLM (Holstein et al., 2011a), a region that innervates preganglionic sympathetic neurons in the intermediolateral cell column of the spinal cord (Card et al., 2006). While the principal neurotransmitter of the pathway from the

RVLM controlling blood pressure is thought to be glutamate (Morrison, 2003), numerous neuroactive molecules have been identified in cells of the RVLM region, notably the C1 catecholaminergic cell group (for review, see Stornetta, 2009). For that reason, several series' of sections through the VNC/RVLM region from sGVS-stimulated and mock-stimulated rats were further processed for immunofluorescence detection of *c-Fos*, glutamate, and tyrosine hydroxylase. *c-Fos* was present in approximately five to eight neuronal nuclei/RVLM/section in the mock-stimulated animals. We observed an approximate threefold increase in *c-Fos* labeling of the RVLM in the sGVS-activated rats. These sGVS-activated neurons in RVLM were large, with long radiating intertwined dendrites (**Figures 8A,B**). Most, but not all, of these sGVS-activated neurons were intensely immunoreactive for tyrosine hydroxylase and approximately half of these were intensely glutamate-immunofluorescent as well (**Figure 8A**).

DISCUSSION

REGIONAL DISTRIBUTION OF sGVS-ACTIVATED VESTIBULAR NEURONS

The present study demonstrates that sGVS activates the immediate early gene *c-fos*, resulting in *c-Fos* protein accumulation in the nuclei of some neurons in SpVN, MVN, SVN, and the parasolitary nucleus. The highest density of *c-Fos*-positive vestibular neurons was observed in MVN. Although we found immunopositive cells distributed throughout the entire rostro-caudal extent of this nucleus, labeled neurons were located predominantly in the caudal and parvocellular regions, and were rarely observed in magno-cellular MVN.

It is noteworthy that neurons in caudal and parvocellular MVN as well as the parasolitary nucleus receive significant otolith input, and send projections to the spinal cord, cerebellum, and inferior olivary complex (for reviews, see Büttner-Ennever, 1992; Barmack, 2003; Highstein and Holstein, 2006; Holstein, 2012). In contrast, magno-cellular MVN receives a preponderance of semi-circular canal-related signals and gives rise to the majority of the vestibulo-ocular projections from MVN (Büttner-Ennever and Gerrits, 2004). Since *c-Fos* protein is not expressed in neurons that are tonically inhibited (Chan and Sawchenko, 1994), and since many vestibulo-ocular neurons receive substantial direct inhibition from cerebellar Purkinje cells and/or vestibular commissural fibers (Holstein et al., 1999; for reviews, see Holstein, 2012; Highstein and Holstein, 2006), it would be surprising if the magno-cellular MVN neurons involved in vestibulo-ocular reflex pathways accumulated *c-Fos* protein. Similarly, vestibulo-spinal and vestibulo-colic neurons did not appear to express *c-Fos* in

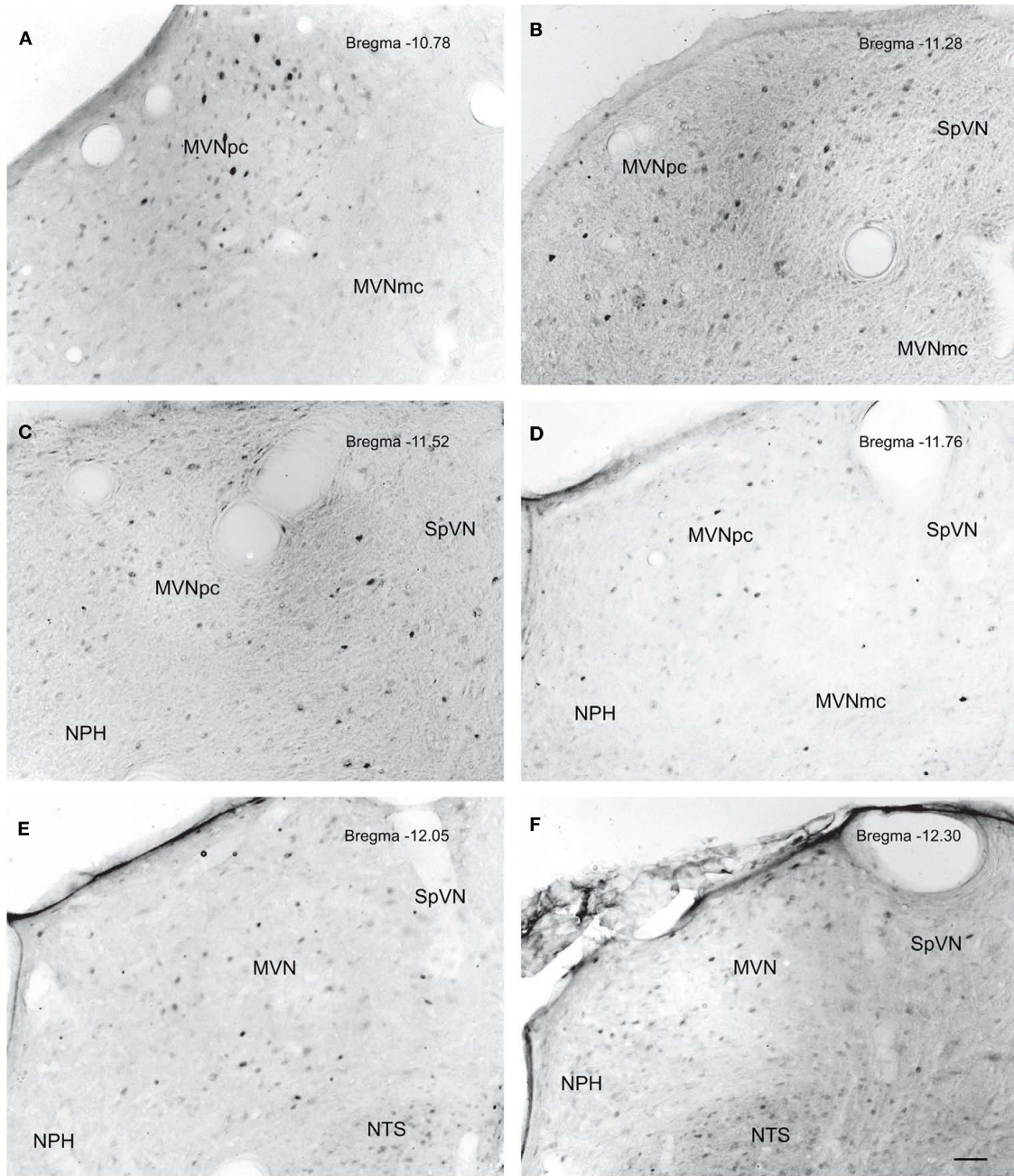


FIGURE 5 | Neurons in MVN activated by sGVS, visualized in vibratome sections processed for c-Fos immunoperoxidase/diaminobenzidine staining. The panels illustrate six rostro-caudal levels of the MVN from the same sGVS-stimulated rat. The images were obtained using the same microscopy and imaging conditions, and were subject to the same adjustments of brightness and contrast (see Materials and Methods). In all panels, the midline is to the left. A dense cluster of immunopositive cells is present in the rostral pole of MVNpc (A,B). The few activated neurons in

MVNmc (A–D) are small diameter cells; none of the larger diameter neurons of this region were c-Fos-positive. c-Fos-stained cells were scattered throughout the caudal spinal vestibular nucleus (B–F). Approximate Bregma levels are indicated in the upper right of each panel. Abbreviations: MVN, medial vestibular nucleus; MVNmc, medial vestibular nucleus, magnocellular division; MVNpc, medial vestibular nucleus, parvocellular division; NTS, nucleus tractus solitarius; SpVN, spinal vestibular nucleus. Scale bar in (F) represents 100 μm, and is for all panels.

our study. This is most likely due to intrinsic cytological differences between sensory and motor pathway neurons since c-Fos is primarily activated by sensory stimuli, and is rarely observed in brainstem neurons involved in motor pathways (Chan and

Sawchenko, 1994). Thus, we would not expect the vestibulo-ocular, -spinal, and -colic motor neurons of the VNC to display c-Fos stain, even though many of these cells are at least transiently activated by sGVS.

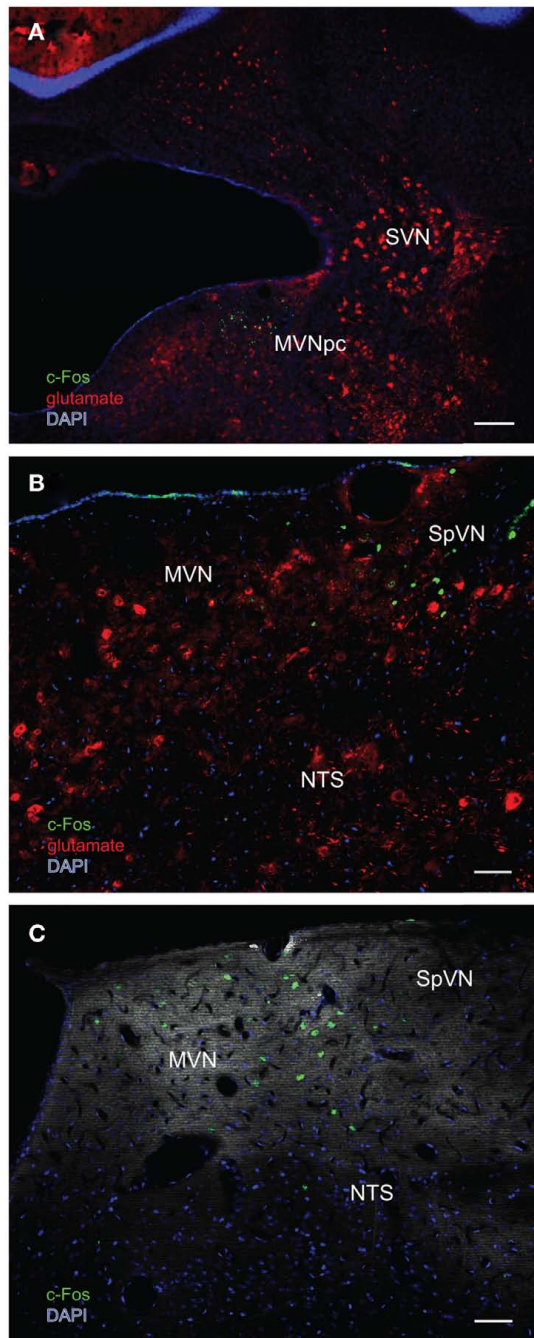


FIGURE 6 | Multiple-label immunofluorescence visualization of c-Fos (green), glutamate (red), and DAPI nuclear stain (blue) in the vestibular nuclei of three different rats stimulated by sGVS. (A) A low magnification overview of rostral medial vestibular nucleus, where there is a discrete cluster of c-Fos immunopositive cells. **(B)** A cluster of sGVS-activated neurons in SpVN. **(C)** sGVS-activated neurons in the parasolitary nucleus. This panel has an irrelevant primary antibody control overlay, in order to better visualize the anatomical landmarks. Scale bars: 200 μm in **(A)**, 50 μm in **(B,C)**. Abbreviations: MVN, medial vestibular nucleus; MVNpc, medial vestibular nucleus, parvocellular division; NTS, nucleus tractus solitarius; SpVN, spinal vestibular nucleus; SVN, superior vestibular nucleus.

In addition to the labeled cells in MVN, we observed sGVS-activated neurons in the caudal, but not rostral, half of SpVN. This localization is consistent with tract-tracing and immunolabeling studies that have identified the caudal half of the VNC, particularly SpVN, and caudal MVN, as the region involved in vestibulo-autonomic control (Balaban and Beryozkin, 1994; Holstein et al., 2011a; for reviews, see Balaban and Yates, 2004; Holstein et al., 2011b). However, vestibular nerve inputs are thought to terminate rostrally and caudally, but not centrally in SpVN (Carleton and Carpenter, 1983, 1984) and not in the caudalmost tip of the nucleus. For that reason, it remains to be determined using a combination of sGVS and VIIIth nerve tract-tracing whether the SpVN neurons that are activated by sGVS are direct recipients of primary afferent innervation, or are downstream participants in descending vestibular pathways.

We consistently observed a small group of c-Fos-immunolabeled neurons in the medial aspect of caudal SVN following sGVS. The SVN is cup-shaped (open end up), with a central area composed of medium sized (30–40 μm diameter) multipolar cell bodies surrounded on three sides by smaller neurons. The central portion of the SVN primarily contains vertical vestibulo-ocular neurons, whereas the parvocellular surround is populated by many neurons with commissural and intra-VNC connections (Mitsacos et al., 1983a,b). As noted above, the vertical vestibulo-ocular neurons of the SVN core are not likely to express c-Fos protein. The parvocellular neurons, in contrast, may participate in vestibulo-autonomic pathways, and/or in polysynaptic unilateral and bilateral intra-VNC connections (Balaban and Yates, 2004). Regardless, it is clear that sGVS activates neurons throughout the entire rostro-caudal extent of the VNC, and not solely the caudal region.

The VNC regions containing sGVS-activated neurons correlate generally, but not precisely, with otolith-recipient areas of the vestibular nuclei demonstrated by traditional tract-tracing methods (Kevetter and Perachio, 1986; Newlands et al., 2002, 2003; for review, see Highstein and Holstein, 2006). For example, Fos-labeled cells were present in the caudal tip of SpVN, which is not thought to receive direct otolith innervation, but there was negligible Fos-related immunolabel in the LVN, although its ventral tier is innervated by otolith nerve fibers. Since sGVS activates the entire vestibular nerve, and since one of the major advantages of c-Fos labeling is its ability to visualize activated neurons at multiple sites of a polysynaptic pathway, a precise correlation between the known otolith nerve projections and c-Fos label associated with an otolith-related stimulus should not be expected. In particular, most regions of the VNC are interconnected bilaterally by commissural fibers (Gacek, 1978; Epema et al., 1988; for review, see Büttner-Ennever, 1992). This system includes homotopic projections between identical areas on either side of the midline and a more widespread system of crossing fibers interconnecting non-homonymous regions of the VNC and related groups. In fact, homotopic commissural pathways have been demonstrated in non-magnocellular regions of MVN, the parvocellular shell of SVN, and parts of SpVN, leaving open the possibility that some of the sGVS-activated neurons visualized in this study are part of the robust vestibular commissural system.

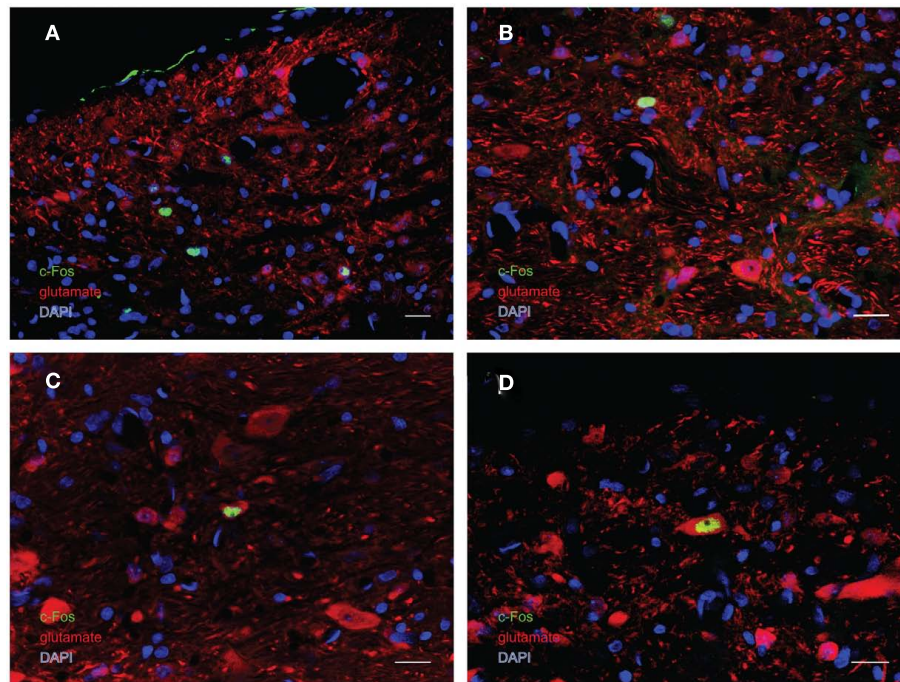


FIGURE 7 | Multiple-label immunofluorescence visualization of c-Fos (green), glutamate (red), and DAPI nuclear stain (blue) in the vestibular nuclei of sGVs-stimulated rats. Three morphological types of vestibular nuclear neurons are activated by sGVs: globular (A,B), multipolar (C), and

fusiform (D). The same three morphological cell types send direct projections from the vestibular nuclei to the RVLM (Holstein et al., 2011a). Approximately one third of the c-Fos-positive neurons showed intense glutamate immunofluorescence (C,D). Scale bars in all panels are 20 μm .

c-FOS EXPRESSION IN THE VESTIBULAR NUCLEI

Previous studies have demonstrated *c-fos* activation in response to various forms of vestibular stimulation. The first reports documented Fos protein in rodent SpVN, MVN, and the γ -group following centripetal acceleration (Kaufman et al., 1991, 1992a,b, 1993). A number of studies have replicated and extended these initial findings, revealing only minor differences in the localization of neurons activated using various stimulation paradigms. In general, the greatest c-Fos expression in response to vestibular stimuli is reported in MVN, SpVN, and SVN, as well as several related cell groups such as nucleus prepositus hypoglossi, the α -group, and the γ -group. For example, sinusoidal linear acceleration in the horizontal (Zhang et al., 2005) and vertical (Lai et al., 2006, 2008) planes activates c-Fos in some neurons within MVN and SpVN, as well as ventral LVN, γ -group, and α -group, but not SVN (Lai et al., 2006, 2008). In contrast, Fos-positive cells are observed in SVN as well as MVN and SpVN following OVAR in rodents (Chen et al., 2003; Lai et al., 2004; Tse et al., 2008) and other species (Gustave Dit Duflo et al., 1999; Baizer et al., 2010), whereas Ferris wheel stimulation results in more widespread c-Fos staining in the VNC (Cai et al., 2007). However, some studies have reported negligible *c-fos* gene expression in the VNC after low (0.25–0.5 Hz) frequency OVAR or head tilt (Lai et al., 2004). Several investigations have utilized galvanic stimuli to activate *c-fos* gene expression in vestibular pathways, and all of these have applied steps of current rather than sinusoidal modulation (Kaufman and Perachio, 1994; Marshburn et al., 1997; Abe et al., 2009). In general, these studies report c-Fos expression in the periventricular zone of MVN, at

an intermediate-rostral level of the nucleus. This location corresponds well with some of the sGVs-activated neurons we observe in rostral MVN (Figure 5A).

c-FOS EXPRESSION IN FUNCTIONALLY RELATED CELL GROUPS

Since c-Fos activation is trans-synaptic, we also observed c-Fos-positive neurons outside the vestibular nuclei, in regions that comprise additional components of the vestibulo-autonomic pathway. As expected, results from the mock-stimulated animals demonstrated a tonic level of *c-fos* activation in NTS and RVLM (for review, see Dampney et al., 2003), two regions that are important for neural control of blood pressure. Tonic activity in these cells presumably reflects the neural signals involved in maintaining homeostatic control of blood pressure under resting conditions. Figure 9 illustrates the relationship between the baroreflex pathways involved in that tonic control, the vestibulo-sympathetic pathway(s) activated in response to postural adjustments, and the convergence of those two pathways in the RVLM. In brief, arterial baroreceptor afferents terminate in NTS, which sends primary projections to the caudal ventrolateral medullary region (CVLM). The CVLM exerts both excitatory and inhibitory influences on RVLM, although the inhibitory connection appears to be most critical for the maintenance of the baroreflex. This pathway is essentially a regulatory feedback mechanism that stabilizes blood pressure. In contrast, signals from the vestibular end organs drive a faster, feed forward mechanism that counteracts the effects of a postural adjustment (for review, see Yates and Bronstein, 2005). This pathway involves direct projections from vestibular neurons

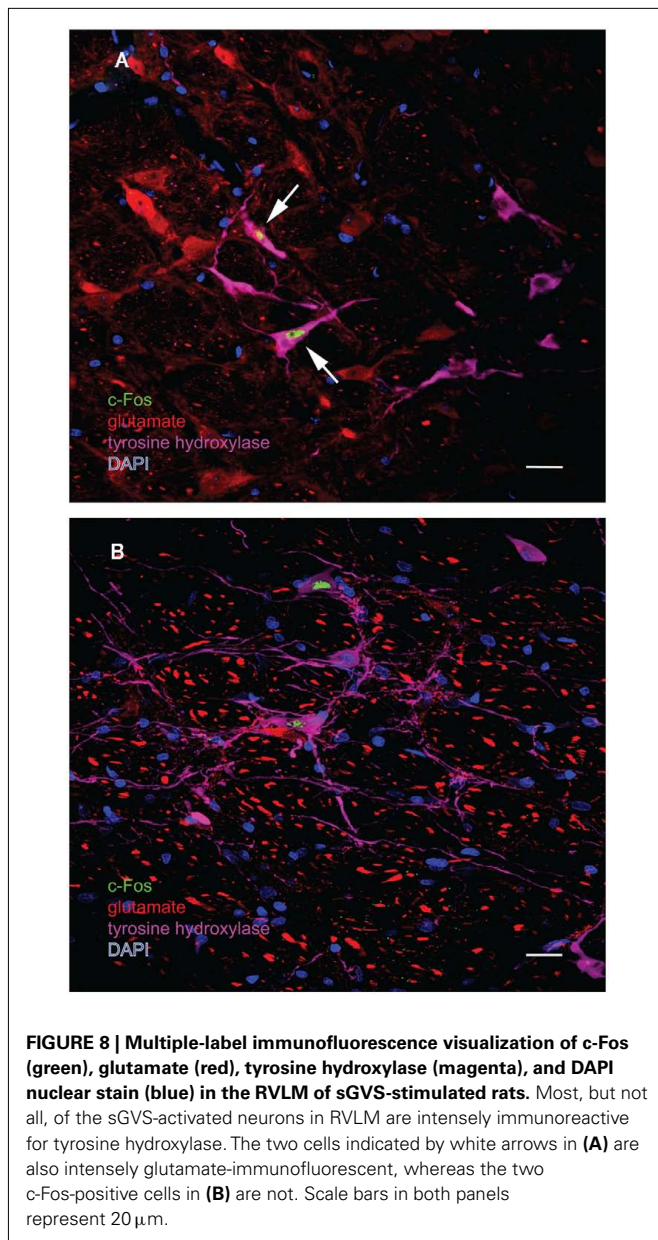


FIGURE 8 | Multiple-label immunofluorescence visualization of c-Fos (green), glutamate (red), tyrosine hydroxylase (magenta), and DAPI nuclear stain (blue) in the RVLM of sGVS-stimulated rats. Most, but not all, of the sGVS-activated neurons in RVLM are intensely immunoreactive for tyrosine hydroxylase. The two cells indicated by white arrows in (A) are also intensely glutamate-immunofluorescent, whereas the two c-Fos-positive cells in (B) are not. Scale bars in both panels represent 20 μm.

in the VNC to the RVLM, as well as indirect pathways via NTS and CVLM.

We observed an approximate threefold increase in the number of c-Fos-positive neurons in the RVLM of sGVS-stimulated rats in comparison with mock-stimulated controls. This finding fits well with previous studies in which Fos-labeled neurons were reported in medullary autonomic nuclei including NTS and RVLM following OVAR (Chen et al., 2003) or centrifugation (Kaufman et al., 1992b). However, since the RVLM receives and processes convergent baroreflex and vestibulo-sympathetic reflex activity, the increase in c-Fos-positive cell number we observe in the RVLM could reflect trans-synaptically activated cells of the vestibulo-sympathetic reflex, and/or neurons of the baroreflex pathway responding to the hypotensive effect of sGVS (Li and Dampney, 1994; for review, see Dampney et al., 2003). Some insight into

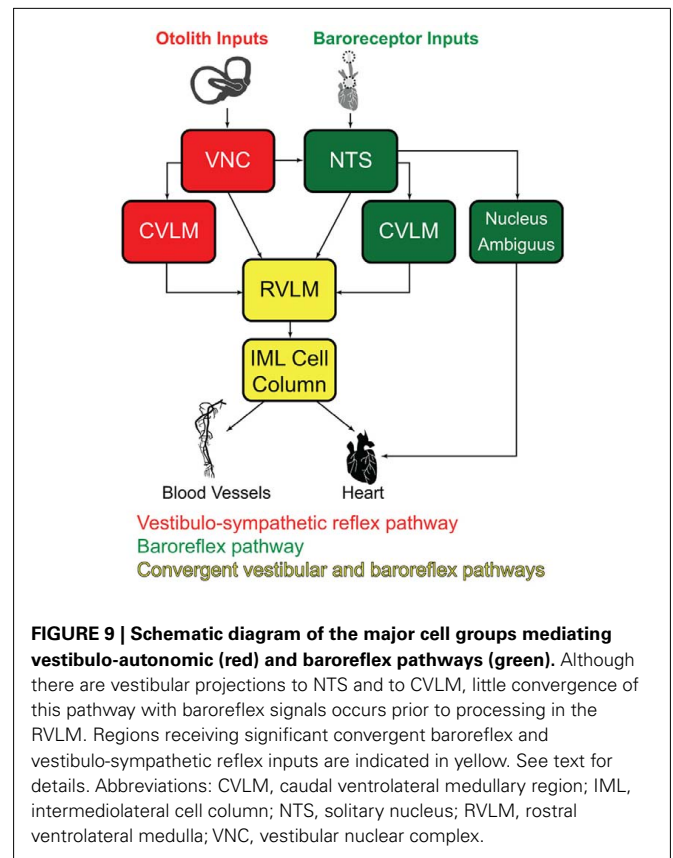


FIGURE 9 | Schematic diagram of the major cell groups mediating vestibulo-autonomic (red) and baroreflex pathways (green). Although there are vestibular projections to NTS and to CVLM, little convergence of this pathway with baroreflex signals occurs prior to processing in the RVLM. Regions receiving significant convergent baroreflex and vestibulo-sympathetic reflex inputs are indicated in yellow. See text for details. Abbreviations: CVLM, caudal ventrolateral medullary region; IML, intermediolateral cell column; NTS, solitary nucleus; RVLM, rostral ventrolateral medulla; VNC, vestibular nuclear complex.

this may be gleaned from our observations of tyrosine hydroxylase localization in most of the c-Fos-positive RVLM neurons. In rabbits, approximately two-thirds of the RVLM neurons activated by drug-induced hypotension synthesize catecholamines (Li and Dampney, 1994). Since we observe a higher frequency of tyrosine hydroxylase labeling in sGVS-activated RVLM neurons than is reported following hypotension alone, it is likely that some of the cells in our study specifically reflect the vestibular stimulus. However, this remains speculative at present, and future quantitative studies assessing the relative levels of neuronal activation in the VNC, NTS, RVLM, and CVLM following sGVS will be necessary to resolve this issue.

VESTIBULAR CELL TYPES ACTIVATED BY sGVS

Multiple-label immunofluorescence studies allowed us to visualize the cell bodies of vestibular neurons with nuclear c-Fos accumulation. To our knowledge, our study is the first cytological and chemoanatomical description of c-Fos-positive cells activated by vestibular stimuli. Three neuronal types were c-Fos-positive: fusiform, multipolar, and globular. We previously observed that these same three types of small diameter cells are retrogradely filled following Fluoro-Gold tracer injections in the RVLM (Holstein et al., 2011a). On that basis, we propose that the small diameter multipolar, fusiform, and globular neurons of the VNC that are activated by sGVS project to the RVLM and serve as the second order neurons of the caudal vestibulo-sympathetic pathway. Approximately one third of those cells show intense glutamate

immunofluorescence, far in excess of the stain reflecting the metabolic pool of cytoplasmic glutamate (Holstein et al., 2004). While these neurons may utilize glutamate for neurotransmission, the transmitter/modulator phenotype(s) of the remaining two-thirds of the sGVS-activated vestibular neurons have yet to be identified. Moreover, it is likely that sGVS may activate vestibular neurons that participate in multiple functional pathways including the vestibulo-spinal and vestibulo-colic reflexes. However, *c-fos* gene expression is not activated in most of these brainstem nuclei associated with motor pathways, and as a result such neurons were not visualized in our study.

VESTIBULAR INFLUENCES ON THE AUTONOMIC NERVOUS SYSTEM

Changes in posture, particularly those involving alterations in head position with regard to gravity, trigger rapid sympathetic nervous system responses. In humans, caloric vestibular stimulation (Cui et al., 1997) and head pitch (Ray and Carter, 2003), as well as GVS (Bent et al., 2006; Grewal et al., 2009; James and Macefield, 2010) influence SNA. Similarly, activation of the otolith organs using OVAR produces an increase in muscle SNA in-phase with the head-up tilt component and a decrease corresponding to the head-down component (Kaufmann et al., 2002). Moreover, linear acceleration (which specifically stimulates the otolith organs) causes transient changes in blood pressure (Cui et al., 1999) that are attenuated in patients with bilateral vestibular deficits (Yates et al., 1999). These studies support the existence of a functional

connection between the vestibular system, particularly the otolith organs, and the sympathetic nervous system in humans, as outlined in **Figure 9**. The present study verifies our observation that sGVS at low frequencies (0.02–0.2 Hz) induces a sudden drop in blood pressure and heart rate in rats (Cohen et al., 2011). These results have been replicated using implanted blood pressure transmitters and various levels of anesthesia (Cohen et al., 2011). As illustrated in **Figure 1**, these autonomic changes can be detected by measuring peripheral blood pressure using PPG.

In summary, the present study examined c-Fos protein accumulation in neurons that are activated by low frequency binaural sGVS in order to identify cell populations putatively involved in the vestibular control of autonomic function. We found c-Fos-positive neurons in the VNC, as well as in the RVLM, and conclude that the localization of c-Fos protein is a reliable marker for neurons of the vestibulo-autonomic pathway. Approximately one third of the c-Fos-labeled vestibular neurons showed intense glutamate immunofluorescence. Future studies will utilize sGVS stimulation and c-Fos labeling to characterize the chemical anatomy of vestibulo-autonomic pathways further.

ACKNOWLEDGMENTS

The authors are grateful to Mr. Tim S. Kang and Dr. Ewa Kukielka for technical assistance with this project. The research was supported by NIH grants DC008846 (GRH), DC004996 (SBY), and Core Center DC05204 (BC).

REFERENCES

- Abe, C., Tanaka, K., Awazu, C., and Morita, H. (2008). Strong galvanic vestibular stimulation obscures arterial pressure response to gravitational change in conscious rats. *J. Appl. Physiol.* 104, 34–40.
- Abe, C., Tanaka, K., Awazu, C., and Morita, H. (2009). Galvanic vestibular stimulation counteracts hypergravity-induced plastic alteration of vestibulo-cardiovascular reflex in rats. *J. Appl. Physiol.* 107, 1089–1094.
- Armstrong, D. M., Ross, C. A., Pickel, V. M., Joh, T. H., and Reis, D. J. (1982). Distribution of dopamine-, noradrenaline-, and adrenaline-containing cell bodies in the rat medulla oblongata: Demonstration by the immunocytochemical localization of catecholamine biosynthetic enzymes. *J. Comp. Neurol.* 212, 173–187.
- Baizer, J. S., Corwin, W. L., and Baker, J. F. (2010). Otolith stimulation induces c-Fos expression in vestibular and precerebellar nuclei in cats and squirrel monkeys. *Brain Res.* 1351, 64–73.
- Balaban, C. D., and Beryozkin, G. (1994). Vestibular nucleus projections to nucleus tractus solitarius and the dorsal motor nucleus of the vagus nerve: potential substrates for vestibular-autonomic interactions. *Exp. Brain Res.* 98, 200–212.
- Balaban, C. D., and Yates, B. J. (2004). “Vestibulo-autonomic interactions: a teleological perspective,” in *The Vestibular System*, eds S. H. Highstein, R. R. Fay, and A. N. Popper (Wein: Springer), 286–342.
- Barmack, N. H. (2003). Central vestibular system: vestibular nuclei and posterior cerebellum. *Brain Res. Bull.* 60, 511–541.
- Bent, L. R., Bolton, P. S., and Macefield, V. G. (2006). Modulation of muscle sympathetic bursts by sinusoidal galvanic vestibular stimulation in human subjects. *Exp. Brain Res.* 174, 701–711.
- Bourassa, E. A., Sved, A. F., and Speth, R. C. (2009). Angiotensin modulation of rostral ventrolateral medulla (RVLM) in cardiovascular regulation. *Mol. Cell. Endocrinol.* 302, 167–175.
- Bradbury, S., and Eggleston, C. (1925). Postural hypotension. A report of three cases. *Am. Heart J.* 1, 73–86.
- Büttner-Ennever, J. A. (1992). “Patterns of connectivity in the vestibular nuclei,” in *Sensing and Controlling Motion: Vestibular and Sensorimotor Function*, eds B. Cohen, D. Tomko, and F. Guedry (New York: New York Academy of Sciences), 363–378.
- Büttner-Ennever, J. A., and Gerrits, N. M. (2004). “Vestibular system,” in *The Human Nervous System*, 2 Edn, eds G. Paxinos and J. K. Mai (London: Elsevier Academic Press), 1212–1240.
- Cai, Y.-L., Ma, W.-L., Li, M., Guo, J.-S., Li, Y.-Q., Wang, L.-G., and Wang, W.-Z. (2007). Glutamatergic vestibular neurons express Fos after vestibular stimulation and project to the NTS and the PBN in rats. *Neurosci. Lett.* 417, 132–137.
- Cai, Y.-L., Want, J.-Q., Chen, X.-M., Li, H.-X., Li, M., and Guo, J.-S. (2010). Decreased Fos protein expression in rat caudal vestibular nucleus is associated with motion sickness habituation. *Neurosci. Lett.* 480, 87–91.
- Card, J. P., Sved, J. C., Craig, B., Raizada, M., Vazquez, J., and Sved, A. F. (2006). Efferent projections of rat rostroventrolateral medulla C1 catecholamine neurons: Implications for the central control of cardiovascular regulation. *J. Comp. Neurol.* 499, 840–859.
- Carleton, S. C., and Carpenter, M. B. (1983). Afferent and efferent connections of the medial, inferior and lateral vestibular nuclei in the cat and monkey. *Brain Res.* 278, 29–51.
- Carleton, S. C., and Carpenter, M. B. (1984). Distribution of primary vestibular fibres in the brainstem and cerebellum of the monkey. *Brain Res.* 294, 281–298.
- Chan, R. K., and Sawchenko, P. E. (1994). Spatially and temporally differentiated patterns of c-fos expression in brainstem catecholaminergic cell groups induced by cardiovascular challenges in the rat. *J. Comp. Neurol.* 348, 433–460.
- Chen, L.-W., Lai, C.-H., Law, H.-Y., Yung, K. K. L., and Chan, Y.-S. (2003). Quantitative study of the coexpression of Fos and N-methyl-D aspartate (NMDA) receptor subunits in otolith-related vestibular nuclear neurons of rats. *J. Comp. Neurol.* 460, 292–301.
- Cirelli, C., Pompeiano, M., D’asciano, P., Arrighi, P., and Pompeiano, O. (1996). c-Fos expression in the rat brain after unilateral labyrinthectomy and its relation to the uncompensated and compensated stages. *Neuroscience* 70, 515–546.
- Cohen, B., Martinelli, G. P., Ogorodnikov, D., Xiang, Y., Raphan, T., Holstein, G. R., and Yakushin, S. B. (2011). Sinusoidal galvanic vestibular stimulation (sGVS) induces a vasovagal response in the rat. *Exp. Brain Res.* 210, 45–55.

- Courjon, J. H., Precht, W., and Sirkin, D. W. (1987). Vestibular nerve and nuclei unit responses and eye movement responses to repetitive galvanic stimulation of the labyrinth in the rat. *Exp. Brain Res.* 66, 41–48.
- Cui, J., Iwase, S., Mano, T., Katayama, N., and Mori, S. (1999). Sympathetic response to horizontal linear acceleration in humans. *J. Gravit. Physiol.* 6, 65–66.
- Cui, J., Mukai, C., Iwase, S., Sawasaki, N., Kitazawa, H., Mano, T., Sugiyama, Y., and Wada, Y. (1997). Response to vestibular stimulation of sympathetic outflow to muscle in humans. *J. Auton. Nerv. Syst.* 66, 154–162.
- Curran, T., and Morgan, J. I. (1995). Fos: an immediate-early transcription factor in neurons. *J. Neurobiol.* 26, 403–412.
- Curthoys, I. S. (2010). A critical review of the neurophysiological evidence underlying clinical vestibular testing using sound, vibration and galvanic stimuli. *Clin. Neurophysiol.* 121, 132–144.
- Dampney, R. A. L., Polson, J. W., Potts, P. D., Hirooka, Y., and Horiuchi, J. (2003). Functional organization of brain pathways subserving the baroreceptor reflex: studies in conscious animals using immediate early gene expression. *Cell. Mol. Neurobiol.* 23, 597–616.
- Darlington, C. L., Lawlor, P., Smith, P. F., and Dragunow, M. (1996). Temporal relationship between the expression of Fos, Jun and Krox-24 in the guinea pig vestibular nuclei during the development of vestibular compensation for unilateral vestibular deafferentation. *Brain Res.* 735, 173–176.
- Dragunow, M., and Faull, R. (1989). The use of c-fos as a metabolic marker in neuronal pathway tracing. *J. Neurosci. Methods* 29, 261–265.
- Durchdewald, M., Angel, P., and Hess, J. (2009). The transcription factor Fos: a Janus-type regulator in health and disease. *Histol. Histopathol.* 24, 1451–1461.
- Epema, A. H., Gerrits, N. M., and Voogd, J. (1988). Commissural and intrinsic connections of the vestibular nuclei in the rabbit: a retrograde labeling study. *Exp. Brain Res.* 71, 129–146.
- Fuller, P. M., Jones, T. A., Jones, S. M., and Fuller, C. A. (2004). Evidence for macular gravity receptor modulation of hypothalamic, limbic and autonomic nuclei. *Neuroscience* 129, 461–471.
- Gacek, R. R. (1978). Location of commissural neurons in the vestibular nuclei of the cat. *Exp. Neurol.* 59, 479–491.
- Goldberg, J. M., Smith, C. E., and Fernandez, C. (1984). Relation between discharge regularity and responses to externally applied galvanic currents in vestibular nerve afferents of the squirrel monkey. *J. Neurophysiol.* 51, 1236–1256.
- Goodchild, A. K., and Moon, E. A. (2009). Maps of cardiovascular and respiratory regions of rat ventral medulla: focus on the caudal medulla. *J. Chem. Neuroanat.* 38, 209–221.
- Grewal, T., James, C., and Macefield, V. G. (2009). Frequency-dependent modulation of muscle sympathetic nerve activity by sinusoidal galvanic vestibular stimulation in human subjects. *Exp. Brain Res.* 197, 379–386.
- Gustave Dit Duflo, S., Gestreau, C., and Lacour, M. (2000). Fos expression in the rat brain after exposure to gravito-inertial force changes. *Brain Res.* 861, 333–344.
- Gustave Dit Duflo, S., Gestreau, C., Tighilet, B., and Lacour, M. (1999). Fos expression in the cat brainstem after unilateral vestibular neurectomy. *Brain Res.* 824, 1–17.
- Herdegen, T., and Leah, J. D. (1998). Inducible and constitutive transcription factors in the mammalian nervous system: control of gene expression by Jun, Fos and Krox, and CREB/ATF proteins. *Brain Res. Rev.* 28, 370–490.
- Highstein, S. M., and Holstein, G. R. (2006). “The anatomy of the vestibular nuclei,” in *Neuroanatomy of the Oculomotor System*, ed. J. A. Büttner-Ennever (Amsterdam: Elsevier), 157–203.
- Holstein, G. R. (2012). “The vestibular system,” in *The Human Nervous System*, 3rd Edn, eds J. Mai and G. Paxinos (London: Elsevier), 1239–1269.
- Holstein, G. R., Friedrich, V. L. J., Kang, T., Kukielka, E., and Martinelli, G. P. (2011a). Direct projections from the caudal vestibular nuclei to the ventrolateral medulla in the rat. *Neuroscience* 175, 104–117.
- Holstein, G. R., Martinelli, G. P., and Friedrich, V. L. J. (2011b). Anatomical observations of the caudal vestibulo-sympathetic pathway. *J. Vestib. Res.* 21, 49–62.
- Holstein, G. R., Martinelli, G. P., and Cohen, B. (1999). The ultrastructure of GABA-immunoreactive vestibular commissural neurons related to velocity storage in the monkey. *Neuroscience* 93, 171–181.
- Holstein, G. R., Martinelli, G. P., Henderson, S. C., Friedrich, V. L. J., Rabbitt, R. D., and Highstein, S. M. (2004). Gamma-aminobutyric acid is present in a spatially discrete subpopulation of hair cells in the crista ampullaris of the toadfish, *Opsanus tau*. *J. Comp. Neurol.* 471, 1–10.
- Hughes, P., and Dragunow, M. (1995). Induction of immediate-early genes and the control of neurotransmitter-regulated gene expression within the nervous system. *Pharmacol. Rev.* 47, 133–175.
- Illing, R.-B., Michler, S. A., Kraus, K. S., and Laszig, R. (2002). Transcription factor modulation and expression in the rat auditory brainstem following electrical intracochlear stimulation. *Exp. Neurol.* 175, 226–244.
- Imholtz, B. P., Wieling, W., Lange-wouters, G. J., and Van Montfrans, G. A. (1991). Continuous finger arterial pressure: utility in the cardiovascular laboratory. *Clin. Auton. Res.* 1, 43–53.
- James, C., and Macefield, V. G. (2010). Competitive interactions between vestibular and cardiac rhythms in the modulation of muscle sympathetic nerve activity. *Auton. Neurosci.* 158, 127–131.
- James, C., Statis, A., and Macefield, V. G. (2010). Vestibular and pulse-related modulation of skin sympathetic nerve activity during sinusoidal galvanic vestibular stimulation in human subjects. *Exp. Brain Res.* 202, 291–298.
- Kaufman, G. D. (2005). Fos expression in the vestibular brainstem: what one marker can tell us about the network. *Brain Res. Rev.* 50, 200–211.
- Kaufman, G. D., Anderson, J. H., and Beitz, A. J. (1991). Activation of a specific vestibulo-olivary pathway by centripetal acceleration in rat. *Brain Res.* 562, 311–317.
- Kaufman, G. D., Anderson, J. H., and Beitz, A. J. (1992a). Brainstem Fos expression following acute unilateral labyrinthectomy in the rat. *Neuroreport* 3, 929–932.
- Kaufman, G. D., Anderson, J. H., and Beitz, A. J. (1992b). Fos-defined activity in rat brainstem following centripetal acceleration. *J. Neurosci.* 12, 4489–4500.
- Kaufman, G. D., Anderson, J. H., and Beitz, A. J. (1993). Otolith-brainstem connectivity – evidence for differential neural activation by vestibular hair cells based on quantification of FOS expression in unilateral labyrinthectomized rats. *J. Neurophysiol.* 70, 117–127.
- Kaufman, G. D., and Perachio, A. A. (1994). Translabyrinthine electrical stimulation for the induction of immediate-early genes in the gerbil brainstem. *Brain Res.* 646, 345–350.
- Kaufman, G. D., Shinder, M. E., and Perachio, A. A. (1999). Correlation of Fos expression and circling asymmetry during gerbil vestibular compensation. *Brain Res.* 817, 246–255.
- Kaufmann, H., Biaggioni, I., Voustantioulou, A., Diedrich, A., Costa, F., Clarke, R., Gizzi, M., Raphan, T., and Cohen, B. (2002). Vestibular control of sympathetic activity. An otolith-sympathetic reflex in humans. *Exp. Brain Res.* 143, 463–469.
- Kevetter, G. A., and Perachio, A. A. (1986). Distribution of vestibular afferents that innervate the sacculus and posterior canal in the gerbil. *J. Comp. Neurol.* 254, 410–424.
- Kim, M. S., Jin, B. K., Chun, S. W., Lee, M. Y., Lee, S. H., Kim, J. H., and Park, B. R. (1997). Effect of MK801 on cFos-like protein expression in the medial vestibular nucleus at early stage of vestibular compensation in uvulonodectomized rats. *Neurosci. Lett.* 231, 147–150.
- Kim, M. S., Kim, J. H., Jin, Y. Z., Kry, D., and Park, B. R. (2002). Temporal changes of cFos-like protein expression in medial vestibular nuclei following arsanilate-induced unilateral labyrinthectomy in rats. *Neurosci. Lett.* 319, 9–12.
- Kitahara, T., Saika, T., Takeda, N., Kiyama, H., and Kubo, T. (1995). Changes in Fos and Jun expression in the rat brainstem in the process of vestibular compensation. *Acta Otolaryngol. Suppl.* 520, 401–404.
- Kitahara, T., Takeda, M., Saika, T., Kubo, T., and Kiyama, H. (1997). Role of the flocculus in the development of vestibular compensation: immunohistochemical studies with retrograde tracing and flocculectomy using Fos expression as a marker in the rat brainstem. *Neurosci. Lett.* 76, 571–580.
- Kovács, K. J. (2008). Measurement of immediate-early gene activation-c-fos and beyond. *J. Neuroendocrinol.* 20, 665–672.
- Lai, C.-H., Tse, Y.-C., Shum, D. K. Y., Yung, K. K. L., and Chan, Y.-S. (2004). Fos expression in otolith-related brainstem neurons of postnatal rats following off-vertical axis rotation. *J. Comp. Neurol.* 470, 282–296.
- Lai, S.-K., Lai, C.-H., Tse, Y.-C., Yung, K. K. L., Shum, D. K. Y., and Chan, Y.-S. (2008). Developmental maturation of ionotropic glutamate receptor subunits in rat vestibular nuclear neurons responsive to vertical linear acceleration. *Eur. J. Neurosci.* 28, 2157–2172.

- Lai, S.-K., Lai, C.-H., Yung, K. K. L., Shum, D. K. Y., and Chan, Y.-S. (2006). Maturation of otolith-related brainstem neurons in the detection of vertical linear acceleration in rats. *Eur. J. Neurosci.* 23, 2431–2446.
- Lau, L. D., Sparto, P. J., Furman, J. M., and Redfern, M. S. (2003). The steady-state postural responses to continuous sinusoidal galvanic stimulation. *Gait Posture* 18, 64–72.
- Li, Y.-W., and Dampney, R. A. L. (1994). Expression of Fos-like protein in brain following sustained hypertension and hypotension in conscious rabbits. *Neuroscience* 61, 613–634.
- MacDougall, H. G., Brizuela, A. E., Burgess, A. M., Curthoys, I. S., and Halmagyi, G. M. (2005). Patient and normal three-dimensional eye-movement responses to maintained (DC) surface galvanic vestibular stimulation. *Otol. Neurotol.* 26, 500–511.
- Marshburn, T. H., Kaufman, G. D., Purcell, I. M., and Perachio, A. A. (1997). Saccul contribution to immediate early gene induction in the gerbil brainstem with posterior canal galvanic or hypergravity stimulation. *Brain Res.* 761, 51–58.
- Mitsacos, A., Reisine, H., and Highstein, S. M. (1983a). The superior vestibular nucleus: an intracellular HRP study in the cat. I. Vestibulo-ocular neurons. *J. Comp. Neurol.* 215, 78–91.
- Mitsacos, A., Reisine, H., and Highstein, S. M. (1983b). The superior vestibular nucleus: an intracellular HRP study in the cat. II. Non-vestibulo-ocular neurons. *J. Comp. Neurol.* 215, 92–107.
- Morgan, J. I., and Curran, T. (1989). Stimulus-transcription coupling in neurons: role of cellular immediate-early genes. *Trends Neurosci.* 12, 459–462.
- Morgan, J. I., and Curran, T. (1991). Stimulus-transcription coupling in the nervous system: involvement of the inducible proto-oncogenes *fos* and *jun*. *Ann. Rev. Neurosci.* 14, 421–451.
- Morrison, S. F. (2003). Glutamate transmission in the rostral ventrolateral medullary sympathetic premotor pathway. *Cell. Mol. Neurobiol.* 23, 761–772.
- Newlands, S. D., Purcell, I. M., Kevetter, G. A., and Perachio, A. A. (2002). Central projections of the utricular nerve in the gerbil. *J. Comp. Neurol.* 452, 11–23.
- Newlands, S. D., Vrabec, J. T., Purcell, I. M., Stewart, C. M., Zimmerman, B. E., and Perachio, A. A. (2003). Central projections of the saccular and utricular nerves in macaques. *J. Comp. Neurol.* 466, 31–47.
- Paxinos, G., Carrive, P., Wang, H., and Wang, P.-Y. (1999). *Chemoarchitectonic Atlas of The Rat Brainstem*. San Diego: Academic Press.
- Paxinos, G., and Watson, C. (1998). *The Rat Brain in Stereotaxic Coordinates*. San Diego: Academic Press.
- Peterson, B. W., Fukushima, K., Hirai, N., Schor, R. H., and Wilson, V. J. (1980). Responses of vestibulospinal and reticulospinal neurons to sinusoidal vestibular stimulation. *J. Neurophysiol.* 43, 1236–1250.
- Pompeiano, O., D'ascanio, P., Centini, C., Pompeiano, M., and Balaban, E. (2002). Gene expression in rat vestibular and reticular structures during and after space flight. *Neuroscience* 114, 135–155.
- Porter, J. D., and Balaban, C. D. (1997). Connections between the vestibular nuclei and regions that mediate autonomic function in the rat. *J. Vestib. Res.* 7, 63–76.
- Ray, C. A., and Carter, J. R. (2003). Review: vestibular activation of sympathetic nerve activity. *Acta Physiol. Scand.* 177, 313–319.
- Saxon, D. W., Anderson, J. H., and Beitz, A. J. (2001). Transtympanic tetrodotoxin alters the VOR and Fos labeling in the vestibular complex. *Neuroreport* 12, 3051–3055.
- Shinder, M. E., Perachio, A. A., and Kaufman, G. D. (2005a). Fos responses to short-term adaptation of the horizontal vestibuloocular reflex before and after vestibular compensation in the Mongolian gerbil. *Brain Res.* 1050, 79–93.
- Shinder, M. E., Perachio, A. A., and Kaufman, G. D. (2005b). VOR and Fos response during acute vestibular compensation in the Mongolian gerbil in darkness and in light. *Brain Res.* 1038, 183–197.
- Shinder, M. E., Ramanathan, M., and Kaufman, G. D. (2006). Asymmetric gene expression in the brain during acute compensation to unilateral vestibular labyrinthectomy in the Mongolian gerbil. *J. Vestib. Res.* 16, 147–169.
- Stornetta, R. L. (2009). Neurochemistry of bulbospinal presympathetic neurons of the medulla oblongata. *J. Chem. Neuroanat.* 38, 222–230.
- Tse, Y.-C., Lai, C.-H., Lai, S.-K., Liu, J. X., Yung, K. K., Shum, D. K., and Chan, Y.-S. (2008). Developmental expression of NMDA and AMPA receptor subunits in vestibular nuclear neurons that encode gravity-related horizontal orientations. *J. Comp. Neurol.* 508, 343–364.
- Voustianiouk, A., Diedrich, A., Ogorodnikov, D., Macdougall, H. G., Raphan, T., Biaggioni, I., Cohen, B., and Kaufmann, H. (2004). Vestibular nerve stimulation modulates muscle sympathetic nerve activity in humans. *Clin. Auton. Res.* 14, 335.
- Voustianiouk, A., Kaufmann, H., Diedrich, A., Raphan, T., Biaggioni, I., Macdougall, H., Ogorodnikov, D., and Cohen, B. (2006). Electrical activation of the human vestibulo-sympathetic reflex. *Exp. Brain Res.* 171, 251–261.
- Watson, S. R., Brizuela, A. E., Curthoys, I. S., Colebatch, J. G., Macdougall, H. G., and Halmagyi, G. M. (1998). Maintained ocular torsion produced by bilateral and unilateral galvanic (DC) vestibular stimulation in humans. *Exp. Brain Res.* 122, 453–458.
- Yates, B. J., Aoki, M., Burchill, P., Bronstein, A. M., and Gresty, M. A. (1999). Cardiovascular responses elicited by linear acceleration in humans. *Exp. Brain Res.* 125, 476–484.
- Yates, B. J., and Bronstein, A. M. (2005). The effects of vestibular system lesions on autonomic regulation: observations, mechanisms, and clinical implications. *J. Vestib. Res.* 15, 119–129.
- Yates, B. J., Grélot, L., Kerman, I. A., Balaban, C. D., Jakus, J., and Miller, A. D. (1994). Organization of vestibular inputs to nucleus tractus solitarius and adjacent structures in cat brain stem. *Am. J. Physiol.* 267, R974–R983.
- Yates, B. J., and Miller, A. D. (1994). Properties of sympathetic reflexes elicited by natural vestibular stimulation: implications for cardiovascular control. *J. Neurophysiol.* 71, 2087–2092.
- Zhang, F. X., Lai, C. H., Tse, Y. C., Shum, D. K. Y., and Chan, Y. S. (2005). Expression of Trk receptors in otolith-related neurons in the vestibular nucleus of rats. *Brain Res.* 1062, 92–100.

Conflict of Interest Statement: The authors declare that the research was conducted in the absence of any commercial or financial relationships that could be construed as a potential conflict of interest.

Received: 17 November 2011; accepted: 04 January 2012; published online: 28 February 2012.

Citation: Holstein GR, Friedrich VL Jr, Martinelli GP, Ogorodnikov D, Yakushin SB and Cohen B (2012) Fos expression in neurons of the rat vestibulo-autonomic pathway activated by sinusoidal galvanic vestibular stimulation. *Front. Neur.* 3:4. doi: 10.3389/fneur.2012.00004

This article was submitted to *Frontiers in Neuro-otology, a specialty of Frontiers in Neurology*.

Copyright © 2012 Holstein, Friedrich Jr, Martinelli, Ogorodnikov, Yakushin and Cohen. This is an open-access article distributed under the terms of the Creative Commons Attribution Non-Commercial License, which permits non-commercial use, distribution, and reproduction in other forums, provided the original authors and source are credited.